# 8 THERMAL COMPENSATION TECHNIQUES

Philip J. Rogers and Michael Roberts
*Pilkington Optronics*
*Wales, United Kingdom*

## 8.1 GLOSSARY

| | |
|---|---|
| $c$ | surface curvature of an optical element |
| $D$ | diameter |
| FN | F-number or focal ratio |
| $f$ | paraxial focal length |
| $G$ | thermo-optical constant (normalized thermal change of OPD) |
| $h$ | (subscript) signifies "pertaining to the optic housing" |
| $i$ | (subscript) number of a specific optical element |
| $j$ | signifies a number of optical elements |
| K | Kelvin |
| $k$ | thermal conductivity |
| $n$ | refractive index |
| OPD | optical path difference |
| $T$ | temperature |
| $t$ | thickness |
| $V$ | Abbe number of a refracting optical material |
| $v$ | spatial frequency |
| $\alpha$ | linear coefficient of thermal expansion |
| $\gamma$ | thermal glass constant (normalized thermal change of optical power) |
| $\Delta$ | small, finite change |
| $\lambda$ | wavelength |
| $\delta$ | infinitely small change of a parameter |
| $\phi$ | optical power (reciprocal of focal length) |

## 8.2 INTRODUCTION

In the following, the thermal effects for which compensation is required are taken to be those that affect the focus and image scale of an optical system. Methods for quantifying and offsetting these effects were described some time ago,[1] similar information being provided by several other authorities.[2,3,4] The thermal compensation techniques described in this chapter, with the exception of intrinsic athermalization, involve either mechanical movement of one or more parts of the optical system, or compensation achieved solely by choice of optical materials. Except in Sec. 8.5 titled "Effect of Thermal Gradients," a homogeneous temperature change of all parts of the optical system is assumed.

Most optical materials undergo a change of refractive index $n$ with temperature $T$, conveniently quoted as a rate of change $\delta n/\delta T$. The usual values of $n$ and $\delta n/\delta T$ given for a material (and assumed in this chapter unless stated otherwise) are those relative to the surrounding air rather than the absolute values with respect to vacuum. Air has a $\delta n/\delta T$ of $-1 \times 10^{-6}$ at $T = 288$ K and 1 atmosphere air pressure for wavelengths between 0.25 and 20 μm:[5] allowance for this must be made when a lens operates in vacuum or in an enclosed space where the number of air molecules per unit volume does not change with temperature. The absolute $\delta n/\delta T$ of an optical material can be found from

$$\left(\frac{\delta n}{\delta T}\right)_{\text{abs}} = n_{\text{air}}\left(\frac{\delta n}{\delta T}\right) + n\left(\frac{\delta n}{\delta T}\right)_{\text{air}} \tag{1}$$

where the value of $n_{\text{air}}$ is approximately 1.0.

## 8.3 HOMOGENEOUS THERMAL EFFECTS

### Thermal Focus Shift of a Simple Lens

The rate of change of the power $\phi$ (reciprocal of the focal length $f$) of an optical element with temperature $T$ can be obtained by differentiating the thin lens power equation $\phi = c(n - 1)$, where $c$ is the total surface curvature of the element. For a linear thermal expansion coefficient $\alpha$ of the material from which the element is formed this gives

$$f = \frac{1}{\phi} \quad \frac{\delta f}{\delta T} = -\frac{1}{\phi^2}\frac{\delta \phi}{\delta T}$$

$$\frac{\delta \phi}{\delta T} = +\phi\left(\frac{\delta n/\delta T}{n-1}\alpha\right) \tag{2}$$

Therefore

$$\frac{\delta f}{\delta T} = -f\left(\frac{\delta n/\delta T}{n-1} - \alpha\right) \tag{3}$$

The material-dependent factor inside the parenthesis in Eqs. (2) and (3) is known as the thermal "glass" constant ($\gamma$) and represents the thermal power change due to an optical material normalized to unit $\phi$ and unit change of $T$. Tables 1 to 3 give $\gamma$ values for a selected number of visual and

**TABLE 1** Optical and Thermal Data for a Number of Visual Waveband Materials

| Schott Optical Glass Plastic Type | Refractive Index, $n_e$* | Abbe Number, $V_e$† | Thermal Glass Constant, $\gamma(\times 10^6)$‡ | Thermo-Optical Constant, $G(\times 10^6)$‡ | Thermal Conductivity, $k(\mathrm{W \cdot m^{-1} \cdot K^{-1}})$ |
|---|---|---|---|---|---|
| FK52 | 1.487 | 81.4 | −27 | +1 | 0.9 |
| FK5 | 1.489 | 70.2 | −11 | +4 | 0.9 |
| BK7 | 1.519 | 64.0 | −1 | +7 | 1.1 |
| PSK53A | 1.622 | 63.2 | −13 | +4 | — |
| SK5 | 1.591 | 61.0 | +1 | +7 | 1.0 |
| BaLKN3 | 1.521 | 60.0 | −3 | +7 | 1.0 |
| BaK2 | 1.542 | 59.4 | −5 | +6 | — |
| SK4 | 1.615 | 58.4 | −2 | +7 | 0.9 |
| LaK9 | 1.694 | 54.5 | −1 | +8 | 0.9 |
| KzFSN4 | 1.617 | 44.1 | +4 | +8 | 0.8 |
| LF5 | 1.585 | 40.6 | −6 | +7 | 0.9 |
| BaSF51 | 1.728 | 37.9 | +8 | +14 | 0.7 |
| LaFN7 | 1.755 | 34.7 | +6 | +12 | 0.8 |
| SF5 | 1.678 | 32.0 | 0 | +11 | — |
| SFN64 | 1.711 | 30.1 | −4 | +9 | — |
| SF6 | 1.813 | 25.2 | +6 | +18 | 0.7 |
| Acrylic§ | 1.497 | 57 | −279 | −71 | 0.2 |
| Polycarbonate§ | 1.590 | 30 | −247 | −68 | 0.2 |

*At $\lambda = 546$ nm.
†Defined as $(n_{546} - 1)/(n_{480} - n_{644})$.
‡At $\lambda = 546$ nm and $T = 20$C.
§Values (except conductivity) from Waxier et al. *Appl. Opt.* **18:**102 (1979).

infrared materials along with the relevant $V$ value (Abbe number) and other data. The much higher level of $\gamma$ for infrared as opposed to glass optical materials indicates that thermal defocus (focus shift) is generally a much more serious problem in the infrared wavebands. The actual value of $\gamma$ varies with both wavelength and temperature due to variations in the value of $\delta n/\delta T$ and $\alpha$. In general, this is unlikely to cause major problems unless a wide wavelength or temperature range is

**TABLE 2** Optical and Thermal Data for Selected 3- to 5-μm Waveband Infrared Materials

| Optical Material | Refractive Index, $n_{4\mu}$ | Abbe Number, $V_{3-5\mu}$ | Thermal "Glass" Constant, $\gamma$ | Thermal Thermo-Optical Constant, $G$ | Conductivity, $k(\mathrm{W \cdot m^{-1} \cdot K^{-1}})$ |
|---|---|---|---|---|---|
| Silicon | 3.43 | $2.4 \times 10^2$ | $+6.3 \times 10^{-5}$ | $+1.7 \times 10^{-4}$ | $1.5 \times 10^2$ |
| KRS5* | 2.38 | $2.3 \times 10^2$ | $-2.3 \times 10^{-4}$ | $-1.5 \times 10^{-4}$ | $5.0 \times 10^{-1}$ |
| AMTIR1† | 2.51 | $1.9 \times 10^2$ | $+3.9 \times 10^{-5}$ | $+9.5 \times 10^{-5}$ | $3.0 \times 10^{-1}$ |
| Zinc selenide | 2.43 | $1.8 \times 10^2$ | $+3.6 \times 10^{-5}$ | $+7.3 \times 10^{-5}$ | $1.8 \times 10^1$ |
| Arsenic trisulfide | 2.41 | $1.6 \times 10^2$ | $-1.9 \times 10^{-5}$ | $+3.4 \times 10^{-5}$ | $1.7 \times 10^{-1}$ |
| Zinc sulfide | 2.25 | $1.1 \times 10^2$ | $+2.6 \times 10^{-5}$ | $+5.2 \times 10^{-5}$ | $1.7 \times 10^1$ |
| Germanium | 4.02 | $1.0 \times 10^2$ | $+1.3 \times 10^{-4}$ | $+4.2 \times 10^{-4}$ | $5.9 \times 10^1$ |
| Calcium fluoride | 1.41 | $2.2 \times 10^1$ | $-5.1 \times 10^{-5}$ | $-1 \times 10^{-6}$ | 9 |
| Magnesium oxide | 1.67 | $1.2 \times 10^1$ | $+1.9 \times 10^{-5}$ | $+2.6 \times 10^{-5}$ | $4.4 \times 10^1$ |

*Thallium bromo-iodide.
†Ge/As/Se chalcogenide from Amorphous Materials Inc.

**TABLE 3** Optical and Thermal Data for Selected 8- to 12-μm Waveband Infrared Materials

| Optical Material | Refractive Index, $n_{10\mu}$ | Abbe Number, $V_{8-12\mu}$ | Thermal "Glass" Constant, $\gamma$ | Thermo-Optical Constant, $\boldsymbol{G}$ | Thermal Conductivity, $k(\mathrm{W \cdot m^{-1} \cdot K^{-1}})$ |
|---|---|---|---|---|---|
| Germanium | 4.00 | $8.6 \times 10^2$ | $+1.2 \times 10^{-4}$ | $+4.1 \times 10^{-4}$ | $5.9 \times 10^1$ |
| Cesium iodide | 1.74 | $2.3 \times 10^2$ | $-1.7 \times 10^{-4}$ | $-5.3 \times 10^{-5}$ | 1 |
| Cadmium telluride | 2.68 | $1.7 \times 10^2$ | $+5.3 \times 10^{-5}$ | $+1.1 \times 10^{-4}$ | 6 |
| KRS5 | 2.37 | $1.7 \times 10^2$ | $-2.3 \times 10^{-4}$ | $-1.6 \times 10^{-4}$ | $5.0 \times 10^{-1}$ |
| AMTIR1 | 2.50 | $1.1 \times 10^2$ | $+3.6 \times 10^{-5}$ | $+9.0 \times 10^{-5}$ | $3.0 \times 10^{-1}$ |
| Gallium arsenide | 3.28 | $1.1 \times 10^2$ | $+7.6 \times 10^{-5}$ | $+2.0 \times 10^{-4}$ | $4.8 \times 10^1$ |
| Zinc selenide | 2.41 | $5.8 \times 10^1$ | $+3.6 \times 10^{-5}$ | $+7.2 \times 10^{-5}$ | $1.8 \times 10^1$ |
| Zinc sulfide | 2.20 | $2.3 \times 10^1$ | $+2.6 \times 10^{-5}$ | $+5.0 \times 10^{-5}$ | $1.7 \times 10^1$ |
| Sodium chloride | 1.49 | $1.9 \times 10^1$ | $-9.5 \times 10^{-5}$ | $-3 \times 10^{-6}$ | 6 |

being considered.[6] Thermal defocus results not only from a change of optical power but also from the thermal expansion coefficient $\alpha_h$ of the housing. Equation (3) can be modified to allow for the effect of the latter:

Single thin lens:
$$\Delta f = -f(\gamma + \alpha_h)\Delta T \tag{4}$$

$j$ thin lenses in contact:
$$\Delta f = -f\left[f\sum_{i-1}^{j}(\gamma_i\phi_i) + \alpha_h\right]\Delta T \tag{5}$$

## Thermal Defocus of a Compound Optical Construction

Consider a homogeneous temperature change in an optical system that comprises two thin-lens groups separated from each other, the normalized thermal power change being the same in each lens group. Taking the thermal defocus calculated from Eq. (4) as unity, then that due to a compound optic comprising two separated components and of the same overall power can be estimated from Fig. 1.[7] The latter shows scaling of thermal defocus with respect to a simple thin lens, relative to front lens/image plane distance (overall length) for three different positions of the second lens group. The graph is divided into three basic lens constructions distinguished from each other by overall optical length and/or the sign of the power of the front lens group.

Figure 1 assumes germanium optics in an aluminum housing but change of either material, while altering values slightly, has no effect on the following two conclusions:

1. Telephoto/inverted telephoto constructions always give more (and Petzval lenses always give less) thermal defocus than an equivalent simple lens.
2. Thermal defocus reduces as the second lens group is moved toward the image plane, irrespective of lens construction: the efficacy of this procedure is limited, however, by the increased imbalance of optical powers between the groups.

The thermal defocus scaling technique could be extended to cover an optic comprising more than two lens groups. This extension has been carried out for the Cooke triplet construction[8] and for a series of separated thin lenses,[6] although only for the case of a zero-expansion housing.

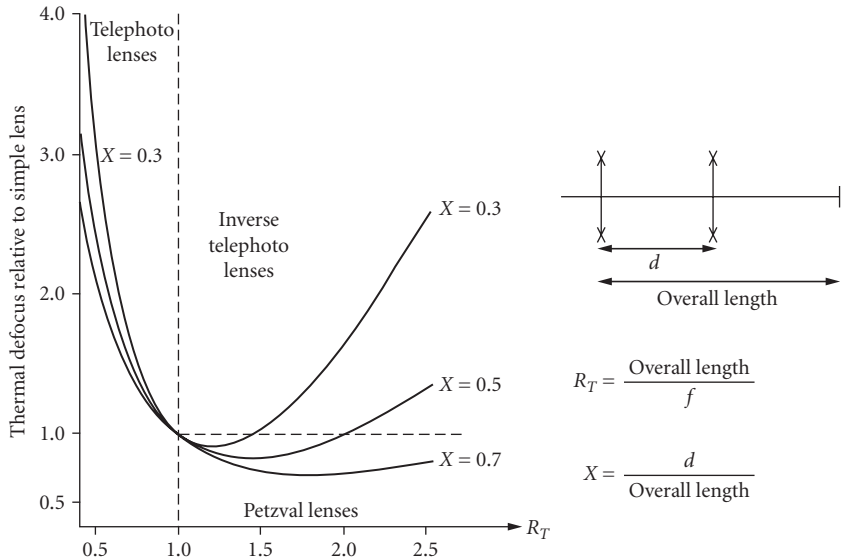


**FIGURE 1** Effect of compound lens construction on thermal defocus. (*From Rogers.*[7])

## 8.4 TOLERABLE HOMOGENEOUS TEMPERATURE CHANGE (NO COMPENSATION)

### Diffraction-Limited Optic

Equation (5) can be used to establish the temperature change $\Delta T$ that will result in a quarter-wave of longitudinal thermal defocus, a reasonable limit for a simple optic that is nominally diffraction-limited. Given an optic of diameter $D$ and focal ratio FN imaging at a mean wavelength of $\lambda$:

Diffraction-based depth of focus:
$$\Delta f = \pm 2\lambda(\text{FN})^2 \tag{6}$$

Combining Eqs. (5) and (6):
$$\Delta T = \pm \frac{2\lambda(\text{FN})}{D\left[f\sum_{i=1}^{j}(\gamma_i \phi_i) + \alpha_h\right]} \tag{7}$$

Figure 2 gives $\Delta T$ against $D$ results for a simple 8- to 12-μm bandwidth germanium optic in an aluminum housing:[9] the curves illustrate the small temperature change that can be tolerated in germanium optics before focus compensation is required. Partial avoidance of this particular problem may be achieved by the replacement of germanium by other infrared optical materials having lower values of $\gamma$: this may also be desirable to reduce high-temperature absorption but generally leads to much greater optical complexity.

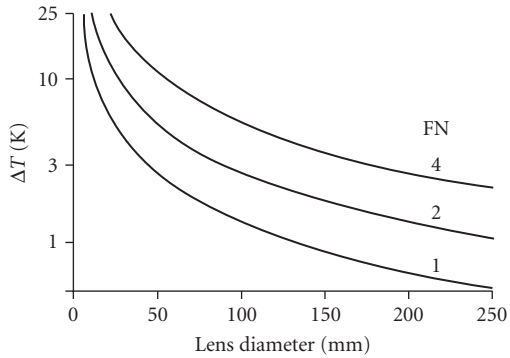


**FIGURE 2** Tolerable temperature change for a simple germanium infrared lens. (*From Rogers.*[9])

### Nondiffraction-Limited Optic

The depth of focus of an optic having a nominal performance far from the diffraction limit is a function of the residual aberration level and balance in the optic as well as its first-order parameters. An estimate related to a cutoff spatial frequency $v$ that gives a reasonable approximation in many cases can be obtained[10] from

Approximate depth of focus:
$$\Delta f = \pm \frac{(\mathrm{FN})}{v} \tag{8}$$

Combining Eqs. (5) and (8):
$$\Delta T = \pm \left\{ Dv \left[ f \sum_{i=1}^{j} (\gamma_i \phi_i) + \alpha_h \right] \right\}^{-1} \tag{9}$$

Notice that, given the approximation of this method, the value of $v$ can be determined by extending a straight line MTF from 1.0 response at zero spatial frequency, through the MTF point of interest, to the intersection of the line with the spatial frequency axis.

## 8.5 EFFECT OF THERMAL GRADIENTS

The previous sections assume a homogeneous temperature change in all parts of the optical system: in situations where steady-state or transient temperature gradients exist, further consideration is required.[1]

Allowance for the effect of steady-state longitudinal gradients can be made by applying a different value of $T$ to each lens group and an average local temperature to each portion of the housing that separates two adjacent lens groups. Transient longitudinal gradients are a more difficult problem and, if severe, may require individual athermalization of each lens group in its own housing domain.

Steady-state or transient radial thermal gradients cause at least a shift of focus position, with the possible addition of a change of aberration correction. A localized radial temperature difference of

$\Delta T$ through the thickness $t$ of a plane-parallel plate will cause a deviation of a ray of light[11] that can be quantified as an optical path difference (OPD):

$$\text{OPD} = t[\alpha(n-1)+\delta n/\delta T]\Delta T \tag{10}$$

The expression in the square bracket is often referred to as the thermo-optical constant $G$ and is an approximate measure of the sensitivity of an optical material to radial gradients. More thorough analysis of the effects produced by radial thermal gradients includes computation of thermally induced stress and consequent anisotropic change of refractive index: in some cases, this may be a significant factor in image degradation.[12–14]

Tables 1 to 3 give values of $G$ for the selected optical materials. Also tabulated is the thermal conductivity $k$, as in many cases $G/k$ is a more appropriate measure of sensitivity given the greater ability of high-conductivity materials to achieve thermal equilibrium.

## 8.6 INTRINSIC ATHERMALIZATION

The need for athermalization can be avoided or minimized for some applications by employing optical power and mounting techniques that are inherently insensitive to temperature change. A concave spherical mirror fabricated from the same material that separates the mirror from its focal plane (e.g., an aluminum mirror in an aluminum housing) is in effect "self-athermalized" for a homogeneous distribution of temperature. The optical performance of a single spherical mirror is limited, but the above principle applies for more complex all-reflective optical constructions employing conic or other aspheric surface forms. A glass spherical mirror, although not thermally matched to an aluminum mounting, may be used as part of a self-athermalized catadioptric afocal in the infrared, a germanium Mangin being used in this case as a secondary mirror lens.[15] The high thermal power change of the negatively powered lens in the germanium Mangin, used in double-pass, compensates for the thermal defocus due to the glass primary, the housing, and the remaining germanium optics in the afocal—Fig. 3.[16]

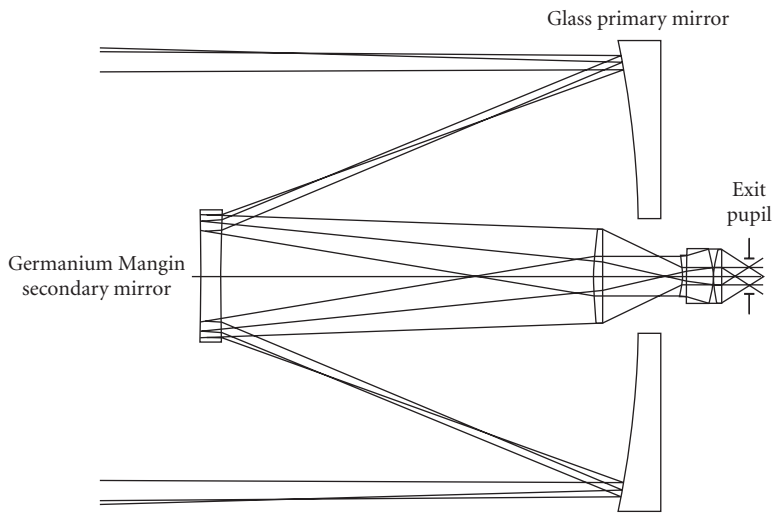


**FIGURE 3** High magnification self-athermalized catadioptric afocal. (*From Norrie.*[16])

An alternative approach to the above is to use glass-ceramic mirrors within a nickel-iron alloy housing, since they can have thermal expansion coefficients approaching zero. A major advantage of this approach is its insensitivity to thermal gradients.

## 8.7 MECHANICAL ATHERMALIZATION

### General

Mechanical athermalization essentially involves some agency moving one or more lens elements by an amount that compensates for thermal defocus—a simple manual option being to use an existing focus mechanism. Automatic methods are, however, preferable in many cases and can be divided into passive or active. Passive athermalization employs an agency, often involving materials (including liquids) with abnormal thermal expansion coefficients, to maintain focus without any powered drive mechanism being required. Automatic active athermalization involves the computation of focus compensation algorithms that are stored (usually electronically) and implemented by a powered device such as an electric motor. The following sections refer to a number of passive and active athermalization methods, although the list is by no means exhaustive.

### Passive Mechanical Athermalization

The principal advantages of passive thermal compensation methods are their relative simplicity and potential reliability. Disadvantages are their inadequate response to transient temperature gradients and, generally, lack of adjustment to allow for errors or unforeseen circumstances. Passive methods are ideal in glass optics[17] where thermal effects are low, although here it is not too difficult to achieve optical athermalization (see later under "Optical Athermalization") except where very low secondary spectrum is required. In the infrared wavebands, where thermal effects are much greater due to the nature of the optical materials, it is difficult to achieve simple passive mechanical athermalization due to the large refocusing movement required, typically $1.5 \times 10^{-4}$ per unit focal length per Kelvin for an aluminum-housed germanium optic. An exception to the above is the combination of silicon and germanium in 3- to 5-μm optics, where thermal defocus results largely from the expansion of the housing. In this case, use of more than one nonmetallic housing material can result in an athermalized optic, even one having two fields of view[18]—Fig. 4.

For infrared cases other than the above, the options are either to provide a mechanism that modifies mechanical expansion effects or to reduce the required refocusing movement by optical means.

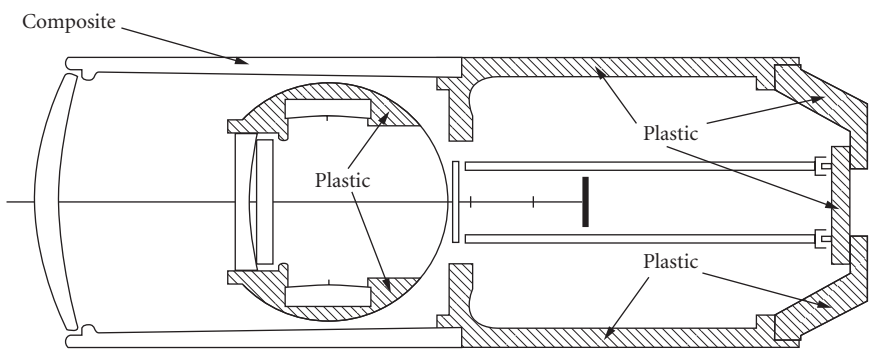


**FIGURE 4** Part composite/part plastic mounting structure used for athermalization of a 3- to 5-μm IR optic. (*From Garcia-Nuñez and Michika.*[18])

THERMAL COMPENSATION TECHNIQUES 

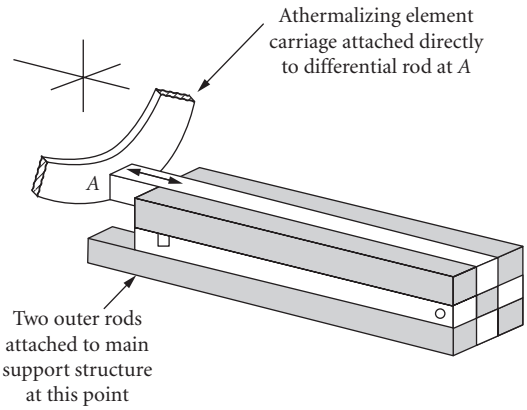


**FIGURE 5** Passive mechanical thermal compensation using differential expansion rods. (*From Povey.*[19])

Examples of the former include[19] a series of linked rods of alternatively high and low expansion coefficient—Fig. 5—and a hydraulic method where the fluid contained in a large-volume reservoir expands into a small-bore cylinder—Fig. 6.

An interesting alternative employs shape-memory metal[20] to provide a large movement over a relatively small temperature range.[19] Another alternative is to employ a geodetic arrangement: in this method[19] an athermalizing adjustment of, for example, the separation between primary and secondary mirrors in a catadioptric, is produced by differing expansion coefficients of the primary mirror

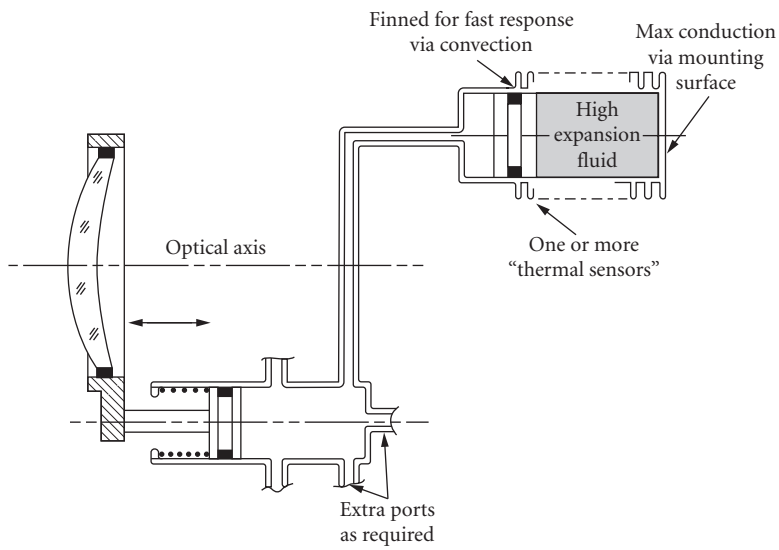


**FIGURE 6** Passive mechanical thermal compensation using high-expansion-fluid thermal sensors. (*From Povey.*[19])

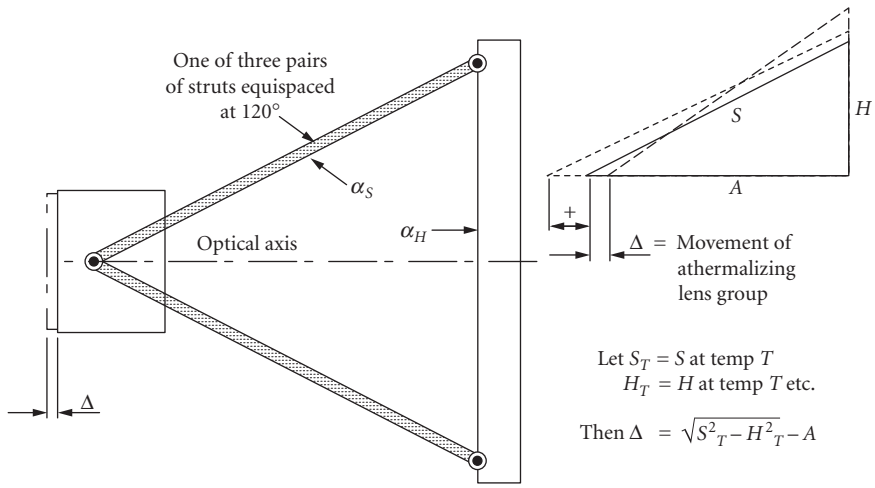


**FIGURE 7** Geodetic support structure for positive or negative thermal compensation movement. (*From Povey.*[19])

mount and the secondary mirror struts—Fig. 7. Where none of the above methods are desirable, the option to reduce the necessary movement may be the only alternative. This may be achieved by an optical layout[9] configured such that the required athermalizing movement is reduced typically by a factor of four, but at the expense of somewhat greater optical complexity—Fig. 8.

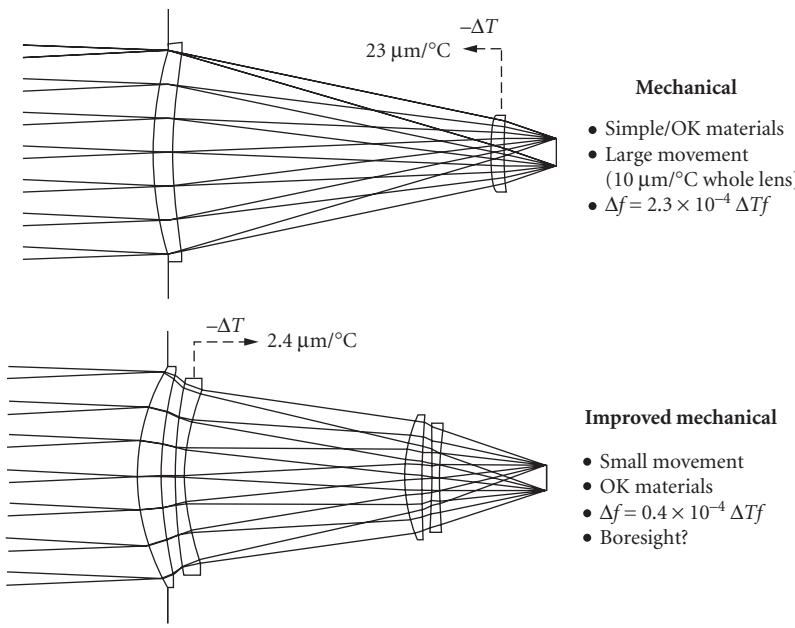


**FIGURE 8** Alternative optical configurations for mechanically athermalized forward looking infrared (FLIR) systems. (*From Rogers.*[9])

THERMAL COMPENSATION TECHNIQUES 

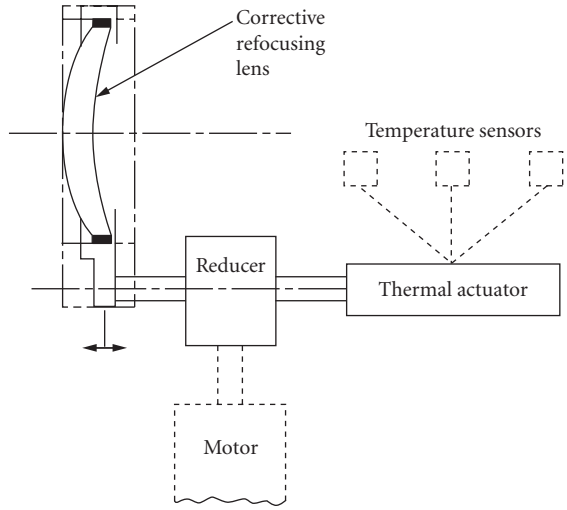


**FIGURE 9** Active electromechanical athermalization—schematic.

## Active Mechanical Athermalization

Active mechanical athermalization in its simplest form can be manual adjustment of a lens element or group for refocusing. For more complex optics, such as multi-field-of-view, a procedure can be specified for manual (or motorized) adjustment of several lens elements to maintain focus over a range of magnifications and temperatures.[21,22] Where automatic athermalization is required, a method can be employed that uses a combination of electronics and mechanics—Fig. 9. One or more temperature sensors located along the body of the optic feed their signals into an algorithm that calculates the required movement of a compensating lens and then initiates the motion. For simplicity, the compensating lens may be that which already provides close-distance focusing, thus requiring only an increase in the range of movement for athermalization. The location of sensors is especially important for infrared optics and should be dependent on the thermal sensitivity variations within the optical system.

Active electromechanical thermal compensation is particularly suitable where transient longitudinal temperature gradients are expected and for multi-field-of-view optics where thermal defocus is dependent on field-of-view setting. The algorithm required for elimination of the effects of a combination of both of the above is complex, but compensation may be accomplished by a single mechanical motion.[23]

A single motion does not, however, guarantee athermalization of image scale, in which case more than one compensatory movement may be required. Two motion athermalization in a zoom or dual-field-of-view infrared telescope can take advantage of the existing mechanisms required for field-of-view change. Also, by utilizing internal lens elements, problems associated with hermetically sealing an external focusing lens element can be avoided.[24–28] In order to maintain stability of aberration correction in infrared zoom telescopes, particularly those having a large zoom range, three-motion athermalization has been proposed.[29,30]

## Active/Passive Athermalization

An improvement over simple manual active athermalization is to include partial passive athermalization. This is best suited to systems that already contain axially moving lens components, for example, a dual-field-of-view infrared telescope[31]—Fig. 10.[32] Here the majority of the athermalization is provided

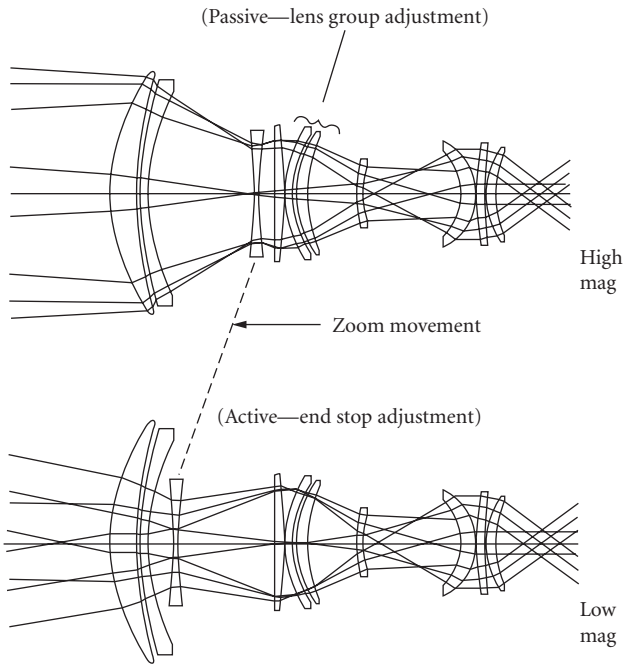


**FIGURE 10** Part active, part passive mechanical athermalization. (*From Roberts.*[32])

by a mechanically passive device that adjusts the position of the rear lens group in the objective. The residual focus error is then corrected by small manual adjustments to the magnification change element. This technique can minimize the change of image scale and aberrations with temperature. A potential problem, however, is the subjective nature of best-focus determination.

### Athermalization by Image Processing

Athermalization by image processing is suitable for some applications. A range of automatic focusing techniques exists but, while this approach has the advantage of not requiring temperature sensors, it does suffer the potential disadvantage of misinterpretation of image information.

## 8.8 OPTICAL ATHERMALIZATION

### General

Athermalization of the focus position of an optical system by choice of refractive materials has been described extensively in the literature.[33–42] The requirements of overall optical power, achromatism, and athermalism demand that three conditions be satisfied for $j$ thin lens elements in contact:

Power: $$\sum_{i=1}^{j} \phi_i = \phi \tag{11a}$$

**TABLE 4** Unity Focal Length Athermal Two-Material Achromatic Combinations

| Material Type | Material Combination | Total Curvatures | Secondary Spectrumt† | Petzval Sum | Normalized Mass |
|---|---|---|---|---|---|
| Optical glasses | BaLKN3 + KzFSN4 | +7.24/−4.49 | $3.6 \times 10^{-4}$ | 0.77 | 2.1 |
| | BaK2 + LaFN7 | +4.43/−1.86 | $4.8 \times 10^{-4}$ | 0.76 | 1.4 |
| | FK5 + LF5 | +4.85/−2.34 | $4.8 \times 10^{-4}$ | 0.73 | 1.3 |
| | PSK53A + SFN64 | +3.06/−1.28 | $5.0 \times 10^{-4}$ | 0.65 | 1.0 |
| | BaLKN3 + BaSF51 | +5.21/−2.35 | $5.2 \times 10^{-4}$ | 0.79 | 1.5 |
| Stabilized optical glasses | SK4 + KzFSN4 | +7.30/−5.64 | $1.8 \times 10^{-4}$ | 0.62 | 2.0‡ |
| | SK5 + SF5* | +3.97/−1.99 | $10.6 \times 10^{-4}$ | 0.67 | 1.0‡ |
| 3- to 5-μm Materials | $As_2S_3$ + MgO | +0.77/−0.12 | $8.6 \times 10^{-4}$ | 0.40 | 0.8§ |

*Thermally invariant housing, all others aluminum.
†Over wavebands of 480 to 644 nm, 546 to 852 nm, and 3 to 5 μm respectively.
‡Relative to SK5/SF5 solution.
§Relative to lowest value in Table 5.
***Source***: Rogers.[43]

Achromatism:
$$\sum_{i=1}^{j} \frac{\phi_i}{V_i} = 0 \tag{11b}$$

Athermalism:
$$\sum_{i=1}^{j} (\gamma_i \phi_i) + \phi \alpha_h = 0 \tag{11c}$$

The presence of three conditions implies the need for three different materials in order to obtain an exact solution. It is possible, however, to find achromatic combinations of two materials that are also athermal, provided that a simple condition is satisfied:[41]

$$V_1(\gamma_1 + \alpha_h) = V_2(\gamma_2 + \alpha_h) \tag{12}$$

Suitable combinations for thin-lens athermal achromats can be found by plotting a range of materials on a graph of $\gamma V$ against $V$, the slope of the line joining a chosen pair representing the required thermal expansion coefficient of the housing.[6]

A number of approximately athermal optical glass achromats exist of which those listed in Table 4[43]—with the exception of the last entry—represent examples with low to moderate secondary spectrum over the visible to near infrared waveband. The data given for these achromats are lens element total curvatures for unity focal length; secondary spectrum (second-order color); thin-lens Petzval sum; and an approximate indication of mass, normalized to the lowest value. The pairing of radiation-stabilized versions of SK5 and SF5, both of which have a low value of $\gamma$ makes a good choice for athermalized space optics in a temperature-invariant mount.[6]

In the infrared wavebands the options are far more limited: at least one 3- to 5-μm waveband two-material athermal combination exists, namely, arsenic trisulfide and magnesium oxide, but there is currently no realistic pairing of materials in the 8- to 12-μm band.

## Athermal Laser Beam Expanders

Many more two-material athermal combinations exist if the requirement for achromatism [Eq. (11*b*)] is removed. This is the situation that occurs with a (preferably) galilean laser beam expander, although here the two lens materials are separated.[44] From Eq. (4), making the thermal defocus $\Delta f$ values equal

and opposite for the two lenses leads to a value for magnification at which two given materials in a specific housing material will provide an athermal beam expander (for a homogeneous temperature distribution):

$$\text{Magnification} = \frac{\gamma_1 + \alpha_h}{\gamma_2 + \alpha_h} \tag{13}$$

## Three-Material Athermal Solutions

Graphical methods have been described that allow investigation of preferred three-material athermalized achromatic solutions.[41] An alternative method is the systematic evaluation of all possible combinations of three materials selected from a short list, each combination being allocated a risk factor dependent on material characteristics and solution sensitivity.[9] The optical powers of the three in-contact thin-lens elements are determined by solving Eq. (11*a* to *c*) which give for a unity focal length:

$$a = \frac{V_1V_2 - V_2V_3}{V_1V_3 - V_2V_3}, \phi_3 = \frac{(1-b)\gamma_1 + b\gamma_2 + \alpha_h}{(1-a)\gamma_1 + a\gamma_2 + \gamma_3} \tag{14a}$$

$$b = \frac{V_2}{V_2 - V_1}, \phi_2 = b - a\phi_3 \tag{14b}$$

$$\phi_1 = 1 - (\phi_2 + \phi_3) \tag{14c}$$

Tables 5 and 6 give a selection of lower-risk three-material solutions, in approximate order of increasing risk, for 3- to 5- and 8 to 12-μm infrared combinations, respectively. The data given are similar to those in Table 4, but the housing is assumed to be aluminum in all cases. Note that these tables are intended as a guide only and are based on currently available material data.

## Athermalization of Separated Components

In many ways, thermal defocus and thermal change of focal length are analogous to longitudinal and lateral chromatic aberration, having the same first-order dependencies. For this reason it has been suggested that a thermal Abbe number, defined as $\gamma^{-1}$,[3] be used to replace the chromatic

**TABLE 5** Unity Focal Length Athermal Three-Material Achromatic Combinations for the 3- to 5-μm Waveband

| Material Combination | Total Curvatures | Petzval Sum | Normalized Mass |
|---|---|---|---|
| Si + Ge + ZnS | +0.72/−0.36/+0.27 | 0.39 | 1.3 |
| ZnSe + Ge + MgO | +1.16/−0.21/−0.06 | 0.51 | 1.8 |
| Si + Ge + KRS5 | +0.69/−0.26/+0.08 | 0.34 | 1.0 |
| [ZnS + MgO + Ge] | +1.28/−0.17/−0.16 | 0.52 | 1.5 |
| AMTIR1 + Ge + Si | +0.56/−0.32/+0.46 | 0.42 | 1.4 |
| Si + MgO + KRS5 | +0.31/−0.08/+0.22 | 0.31 | 1.1 |
| ZnSe + ZnS + Ge | +1.80/−0.69/−0.23 | 0.50 | 2.8 |
| Si + $CaF_2$ + KRS5 | +0.32/−0.25/+0.24 | 0.29 | 1.1 |

[ ] Low residual high-order chromatic aberration.

**TABLE 6** Unity Focal Length Athermal Three-Material Achromatic Combinations for the 8- to 12-μm Waveband

| Material Combination | Total Curvatures | Petzval Sum | Normalized Mass |
|---|---|---|---|
| KRS5 + ZnSe + Ge | +0.34/−0.15/+0.25 | 0.30 | 1.0 |
| ZnSe + ZnS + Ge | +2.05/−0.92/−0.26 | 0.50 | 2.5 |
| GaAs + ZnS + KRS5 | +0.38/−0.20/+0.26 | 0.31 | 1.0 |
| AMTIR1 + ZnS + Ge | +1.42/−0.35/−0.24 | 0.48 | 1.3 |
| {CdTe + ZnSe + KRS5} | +0.72/−0.37/+0.22 | 0.37 | 1.5 |
| GaAs + ZnSe + KRS5 | +0.68/−0.71/+0.33 | 0.25 | 1.8 |
| [AMTIRI + ZnSe + KRS5] | +1.19/−0.72/+0.16 | 0.39 | 1.9 |
| [Csl + NaCl + GaAs] | +0.68/−0.32/+0.29 | 0.38 | 1.1 |

{ } Very high transmission.
[ ] Low residual high-order chromatic aberration.

Abbe number ($V$ value) in the usual chromatic aberration equations. Thermal expansion of the housing—obviously not present in chromatic calculations—does, however, complicate the situation a little.

In equations thus far, $\Delta f$ has meant both thermal defocus and focal length change, as numerically these are the same for a thin lens. For separated components, rules similar to those for chromatic aberration apply, for example, two separated thin-lens groups—such as those described by Fig. 1—must be individually athermalized if both types of thermal "aberration" are to be corrected simultaneously. More complex optics (for example, multistage) may have transfer of thermal aberration between constituent lens groups but may still be corrected simultaneously for thermal focus shift and focal length change as a whole. This procedure can, however, lead to one lens group requiring excessive optical powers in order to achieve full overall correction—transient longitudinal thermal gradients may also cause problems.

### Use of Diffractive Optics in Optical Athermalization

The term "hybrid optic" is generally used to signify a combination of refractive and diffractive means in an optical element. The diffractive part of the hybrid is usually a transmission hologram which for high efficiency would be of surface relief form, the surface structure being machined or etched onto the refractive surface.[45] The diffractive surface acts as a powered diffraction grating, producing large amounts of chromatic aberration which could be employed in an optic where a lightweight optically athermalized combination of two materials could be chosen without regard to achromatism: residual chromatic aberration could then be corrected by the hologram.[46]

## 8.9 REFERENCES


1. J. W. Perry, *Proc. Phys. Soc.,* vol. 55, 1943, pp. 257–285.
2. J. lohnson and J. H. Jeffree, U.K. Patent No. 561 503, 1942 U.K. priority.
3. D. S. Grey, *J. Opt. Soc. Am.,* vol. 38, 1948, pp. 542–546.
4. D. S. Volosov, *Opt. Spectrosc.,* U.S.S.R., vol. 4, pp. 663–669 and pp. 772–778, vol. 5, 1958, pp. 191–199.
5. R. Penndorf, *J. Opt. Soc. Am.,* vol. 47, 1957, pp. 176–182.
6. H. Köhler and F. Strähle, *Space Optics,* B. J. Thompson and R. R. Shannon (eds.), National Academy of Sciences, 1974, pp. 116–153
7. P. J. Rogers, *SPIE Critical Reviews,* vol. CR38, 1991, pp. 69–94.
8. L. R. Estelle, *SPIE,* vol. 237, 1980, pp. 392–401.

9. P. J. Rogers, *SPIE,* vol. 1354, 1990, pp. 742–751.
10. M. Laikin, *Lens Design,* Marcel Dekker, New York, 1991, p. 28.
11. G. G. Slyusarev, *Opt. Spectrosc.,* U.S.S.R., vol. 6, 1959, pp. 134–138.
12. W. H. Turner, *Optical Sciences Center,* vol. 4, University of Arizona, Tucson, Arizona, 1970, pp. 123–125.
13. V. M. Mit'kin and O. S. Shchavelev, *Sov. J. Opt. Tech.,* vol. 40, 1973, pp. 558–561.
14. F. Reitmayer and H. Schroeder, *Appl. Opt.,* vol. 14, 1975, pp. 716–720.
15. P. J. Rogers, *SPIE,* vol. 147, 1978, pp. 141–148; and U.K. Patent No. 2,030,315.
16. D. G. Norrie, *Opt. Eng.,* vol. 25, 1986, pp. 319–322.
17. J. Angénieux et al., *SPIE,* vol. 399, 1983, pp. 446–448.
18. D. S. Garcia-Nuñez and D. Michika, *SPIE,* vol. 1049, 1989, pp. 82–85.
19. V. Povey, *SPIE,* vol. 655, 1986, pp. 142–153.
20. A. D. Michael and W. B. Hart, *Metallurgist and Materials Technologist,* August 1980, pp. 434–440.
21. G. V. Thompson, U.S. Patent No. 4,148,548, 1976 U.K. priority.
22. P. J. Rogers and G. N. Andrews, *SPIE,* vol. 99, 1976, pp. 163–175.
23. P. M. Parr-Burman and A. Gardam, *SPIE,* vol. 590, 1985, pp. 11–17.
24. I. A. Neil and W. McCreath, U.K. Patent No. 2,141,260, 1983 U.K. priority.
25. I. A. Neil, U.S. Patent No. 4,659,171, 1984 U.K. priority.
26. I. A. Neil and M. Y. Turnbull, *SPIE,* vol. 590, 1985, pp. 18–29.
27. P. Nory, *SPIE,* vol. 590, 1985, pp. 30–39.
28. P. M. Parr-Burman and P. Madgwick, *SPIE,* vol. 1013, 1988, pp. 92–99.
29. R. C. Simmons and P. A. Blaine, *SPIE,* vol. 916, 1988, pp. 19–26.
30. M. Shechterman, *SPIE,* vol. 1442, 1990, pp. 276–285.
31. M. Roberts and P. R. Crew, U.K. Patent No. 2,201,011, 1987 U.K. priority.
32. M. Roberts, *SPIE,* vol. 1049, 1989, pp. 72–81.
33. C. B. Estes, U.S. Patent No. 3,205,774, 1961 U.S. priority.
34. R. C. Gibbons, *ERIM Report No. 120200-I-X*, 1976, p. 71.
35. K. Straw, *SPIE,* vol. 237, 1980, pp. 386–391.
36. M. O. Lidwell, U.S. Patent No. 4,494,819, 1980 U.K. priority.
37. T. H. Jamieson, *Opt. Eng.,* vol. 20, 1981, pp. 156–160.
38. I. A. Neil, U.S. Patent No. 4,505,535, 1982 U.K. priority.
39. M. Roberts, U.S. Patent No. 4,679,891, 1984 U.K. priority.
40. P. J. Rogers, Thermal Imaging course notes, Institute of Optics, Summer School on Lens Design, Rochester, 1988 (unpublished).
41. J. L. Rayces and L. Lebich, *SPIE,* vol. 1354, 1990, pp. 752–759.
42. M. Yatsu et al., *SPIE,* vol. 1354, 1990, pp. 663–668.
43. P. J. Rogers, *SPIE,* vols. 1780 and 1781, 1992, pp. 36–48.
44. J. M. Palmer, U.K. Patent No. 2,194,072, 1986 U.K. priority.
45. G. J. Swanson and W. B. Veldkamp, *Opt. Eng.,* vol. 28, 1989, pp. 605–608.
46. P. J. Rogers, *SPIE,* vol. 1573, 1992, pp. 13–18.